Emergence rate of the time-domain Green's function from the ambient noise cross-correlation function

Karim G. Sabra,[a] Philippe Roux, and W. A. Kuperman
Marine Physical Laboratory, Scripps Institution of Oceanography, La Jolla, California 92093-0238

(Received 20 June 2005; revised 25 August 2005; accepted 8 September 2005)

It has been demonstrated experimentally and theoretically that an estimate of the Green's function between two receivers can be obtained from the time derivative of the long-time average ambient noise function cross-correlation function between these two receivers. The emergence rate of the deterministic coherent arrival times of the cross-correlation function, which yield an estimate of the Green's function, from the recordings of an isotropic distribution of random noise sources is studied by evaluating the amplitude of the variance of the cross-correlation function. The leading term in the expression of the variance depends on the recorded energy by both receivers and the time-bandwidth product of the recordings. The variance of the time derivative of the correlation function has a similar dependency. These simple analytic formulas show a good agreement with the variance determined experimentally for the correlation of ocean ambient noise for averaging time varying from 1 to 33 min. The data were recorded in shallow water at a depth of 21-m water depth in the frequency band [300–530 Hz] for receivers separation up to 28 m. © *2005 Acoustical Society of America.* [DOI: 10.1121/1.2109059]

PACS number(s): 43.30.Nb, 43.50.Rq, 43.60.Tj [RLW] Pages: 3524–3531

I. INTRODUCTION

Experimental and theoretical analysis have shown that the arrival-time structure of the time-domain Green's function (TDGF) can be estimated from the time derivative of the time-averaged ambient noise cross-correlation function (NCF) in various environments and frequency ranges of interest: helioseismology,[1] ultrasonics,[2–6] underwater acoustics,[7–9] and seismology.[10–14] The physical process underlying this noise cross-correlation technique is similar for all these environments. Initially, the small coherent component of the noise field at each receiver is buried in the spatially and temporally incoherent field produced by the distribution of noise sources. The coherent wavefronts emerge from a correlation process that accumulates contributions over time from noise sources whose propagation path passes through both receivers.

Based on theoretical and experimental results,[6,8,11,12,15] the following relationship between the TDGF between two receivers a and b, located respectively at $\vec{r}_a$ and $\vec{r}_b$, and the time derivative of the expected value of the NCF $\langle C_{a,b}(\tau)\rangle$ can be stated:

$$\frac{d\langle C_{a,b}(\tau)\rangle}{d\tau} \approx -G(\vec{r}_a,\vec{r}_b;\tau) + G(\vec{r}_b,\vec{r}_a;-\tau). \tag{1}$$

In Eq. (1), the terms on the rhs are respectively (1) the TDGF, which comes from noise events that propagate from receiver a to b and yields a positive correlation time-delay τ, and (2) the time-reversed TDGF, which comes from noise events that propagate from receiver b to a and yields a negative correlation time delay $-\tau$. Thus, for a uniform noise source distribution or a fully diffuse noise field, the derivative of the NCF is an antisymmetric function with respect to time, the NCF itself being a symmetric function. The exact relationship (in amplitude and arrival times) between the time derivative of the time-averaged NCF and the deterministic TDGF generally depends of specific noise source distribution and the environment. For instance, the source directionality creates shading of the wavefronts of the NCF with respect to the true TDGF.[7,8]

Experimental results typically show that a sufficiently long time-averaging interval (as long as environmental changes do not modify the acoustic propagation paths) and a spatially homogeneous noise distribution helps in estimating the arrival-time structure of the TDGF from this correlation process.[2,7,9] Determining precisely the dependence of the emergence rate of the coherent wavefronts of the NCF on the noise recording duration and the various environment parameters is essential for practical applications. This emergence rate (or convergence rate) can be defined based on the variance of the NCF. Indeed, the variance corresponds to the fluctuations of the NCF around its expected value whose time derivative is an estimate of the TDGF.

An upper bound on the variance of the NCF has been previously derived in the case of a homogeneous medium with embedded scatterers.[11] Furthermore, a formulation of the variance of the NCF for open systems and closed systems based on a modal expansion of the Green's function for the case of local diffuse fields has also been presented.[16] In this paper, an expression of the variance of the NCF is derived independently of the particular expression of the Green's function (free space, modal or rays expansion,…) for the environment of interest (e.g., ultrasonic experiments, underwater acoustics, seismology,…) and of the shape of the noise spectrum. This resulting analytic formula variance of the NCF is derived assuming only (1) an isotropic distribution of impulsive random noise sources and (2) a finite duration

[a]Electronic mail: ksabra@mpl.ucsd.edu

 © 2005 Acoustical Society of America

Green's function, which is true for any physical systems in the presence of attenuation. Furthermore, this formulation is readily extended to the variance of the time derivative of the NCF. In the case of a white noise model and finite bandwidth recordings, this analytic formula reduces to previous derivations when using a homogeneous free-space model[11] or a modal expansion of the Green's function.[16,17] The analytic results are compared to the variance of experimental NCF obtained from ocean noise recordings of various duration up to 33 min in the frequency band [300–530 Hz]. The ambient noise data were recorded on a bottom array in shallow water during the Adaptive Beach Monitoring (ABM 95) experiment.[9]

This article is divided into five sections. Section II presents a time-domain formulation of the NCF. Section III derives an analytic formula for the variance of the NCF and the time derivative of the NCF. Section IV provides an overview of the ABM 95 experiment and discusses the ambient NCFs obtained. Experimental measures of the variance of the NCF are then compared to the theoretical predictions of Sec. III. Section V summarizes the findings and conclusions drawn from this study.

II. FORMULATION OF THE AMBIENT NOISE CROSS-CORRELATION FUNCTION (NCF)

The signal recorded at two receivers a and b located respectively at $\vec{r}_a$ and $\vec{r}_b$ from a single random noise source (located at $\vec{r}_1$, broadcasting at a time t_1) is fully determined by the TDGF in the environment of interest, which for instance is noted $G(\vec{r}_1,\vec{r}_a;t-t_1)$ between this random source and receiver a.[18] Here, the causality requires that the noise source in $(\vec{r}_1;t_1)$ that contributes to the pressure field in a at a given time t satisfy the condition $t>t_1$. We assumed that the (impulse) response of both receiver a and b is embedded in the TDGF. The random impulse noise sources are assumed to follow a shot-noise model which is appropriate for broadband noise sources realizations.[8,19] In this model each noise source broadcasts, at a random time t_1, a signal $S(\vec{r}_1;t_1)$. The resulting noise waveforms are represented by a random pulse train consisting of similarly shaped pulses randomly distributed in time. In the case of white noise, the noise sources have a flat frequency spectrum.[19] In the present context, *random* means that the discrete events giving rise to the pulses are temporally and spatially incoherent in the limit of infinite recording time and infinite bandwidth (due to the impulsive nature of the sources) and have the same amplitude Q (whose unit depends on the variable being measured, e.g., pressure or displacement). The statistical law governing the distribution of the events in time is the Poisson probability density function and has a creation rate ν ($\mathrm{m}^{-3}\mathrm{s}^{-1}$) per unit time per unit volume. Hence the second-order moment of the uncorrelated noise sources can be written as[8,15]

$$\langle S(\vec{r}_1;t_1)S(\vec{r}_2;t_2)\rangle = \nu Q^2 \delta(\vec{r}_1-\vec{r}_2)\cdot\delta(t_1-t_2). \tag{2}$$

In practice, the contribution of the noise sources is limited in range due to attenuation. The total field at receiver a location is then

$$P(\vec{r}_a;t) = \int_{-\infty}^{+\infty} d\vec{r}_1 \int_{-\infty}^{t} dt_1 S(\vec{r}_1;t_1) G(\vec{r}_1,z_1,\vec{r}_a,z_a;t-t_1). \tag{3}$$

In a stationary medium, the temporal NCF $C_{a,b}(\tau)$ between the signals recorded by both receivers is defined as

$$C_{a,b}(\tau) = \int_{-T_r/2}^{T_r/2} dt P(\vec{r}_a;t) P(\vec{r}_b;t+\tau). \tag{4}$$

In practice, the NCF is constructed from ensemble averages, denoted by $\langle\ \rangle$, over realizations of the noise source signals $S(\vec{r}_1;t_1)$. The integration over the variable t, i.e., the recording time for receiver a and b, corresponds to an accumulation of noise sources events over time. In practice, the signals recorded by receivers a and b are correlated only over a finite interval T_r (including both positive and negative time delays).[15] For short correlation time τ (i.e., $\tau \ll T_r$) with respect to the recording duration at each receiver T_r, the tapering of the NCF which occurs otherwise on the edges of the finite correlation interval, i.e., for $\tau \approx T_r$, can be neglected.

Assuming a noise statistical model given by Eq. (2), using Eq. (3), and after performing a change of variables $u = t-t_1$, the ambient noise cross-correlation function defined in Eq. (4) can be expressed as

$$\langle C_{a,b}(\tau)\rangle = \nu Q^2 T_r \int_{-\infty}^{+\infty} d\vec{r}_1 \int_{0}^{+\infty} du G(\vec{r}_1,\vec{r}_a;u) G(\vec{r}_1,\vec{r}_b;\tau+u). \tag{5}$$

The TDGF has typically a finite temporal length noted T_{Green}, i.e., the time duration after which no more multipath arrivals can be detected. In practice, the value of the parameter T_{Green} depends on absorption, on the ambient noise level, and on the receiver dynamics (and sensitivity). Hence the relationship between the TDGF between the receivers a and b and the time derivative of the expected value of the NCF given by Eq. (1) shows that after sufficient averaging of the NCF and for time delay $\tau > T_{\mathrm{Green}}$, only small residual fluctuations are measured by the NCF. The level of these fluctuations corresponds to the square of the variance (or standard deviation) of this noise correlation process noted $\mathrm{Var}(C_{a,b}(\tau))$. A measure of the variance $\mathrm{Var}(C_{a,b}(\tau))$ gives an estimate of the residual error done when approximating the TDGF by the time derivative of the NCF and is thus a key quantity to evaluate. Based on the time-domain formalism developed in this section, a simplified formulation of the variance of this noise correlation process $\mathrm{Var}(C_{a,b}(\tau))$ is developed in the following section for an arbitrary TDGF with a finite temporal length T_{Green}.

III. VARIANCE OF THE AMBIENT NOISE CORRELATION FUNCTION. THEORY

A. Variance of the NCF

The variance of the ambient noise cross-correlation process, i.e., the square of the mean level of the fluctuations, is defined as[16]

$$\mathrm{Var}(C_{a,b}(\tau)) = \langle C_{a,b}^2(\tau)\rangle - \langle C_{a,b}(\tau)\rangle^2, \tag{6}$$

where the expected value of $\langle C_{a,b}(\tau)\rangle$ is given by Eq. (5). By combining Eqs. (3) and (4), the expression of $C_{a,b}^2(\tau)$ can be expanded as

$$\begin{aligned} C_{a,b}^2(\tau) = & \int_{-T_r/2}^{T_r/2} dt \int_{-T_r/2}^{T_r/2} d\tilde{t} \int_{-\infty}^{+\infty} d\vec{r}_1 \int_{-\infty}^{+\infty} d\vec{r}_2 \int_{-\infty}^{+\infty} d\vec{r}_3 \\ & \times \int_{-\infty}^{+\infty} d\vec{r}_4 \int_{-\infty}^{t} dt_1 \int_{-\infty}^{t} dt_2 \int_{-\infty}^{\tilde{t}} dt_3 \int_{-\infty}^{\tilde{t}} dt_4 \\ & \times S(\vec{r}_1;t_1) S(\vec{r}_2;t_2) S(\vec{r}_3;t_3) S(\vec{r}_4;t_4) \\ & \times G(\vec{r}_1,\vec{r}_a;t-t_1) G(\vec{r}_2,\vec{r}_b;\tau+t-t_2) \\ & \times G(\vec{r}_3,\vec{r}_a;\tilde{t}-t_3) G(\vec{r}_4,\vec{r}_b;\tau+\tilde{t}-t_4). \end{aligned} \tag{7}$$

Assuming that the random sources are temporally and spatially incoherent with Gaussian statistics, the expression of the fourth-order moment $\langle S(\vec{r}_1;t_1) S(\vec{r}_2;t_2) S(\vec{r}_3;t_3) S(\vec{r}_4;t_4)\rangle$ reduces to

$$\begin{aligned} & \langle S(\vec{r}_1;t_1) S(\vec{r}_2;t_2) S(\vec{r}_3;t_3) S(\vec{r}_4;t_4)\rangle \\ & \quad = \langle S(\vec{r}_1;t_1) S(\vec{r}_2;t_2)\rangle \langle S(\vec{r}_3;t_3) S(\vec{r}_4;t_4)\rangle \\ & \qquad + \langle S(\vec{r}_1;t_1) S(\vec{r}_3;t_3)\rangle \langle S(\vec{r}_2;t_2) S(\vec{r}_4;t_4)\rangle \\ & \qquad + \langle S(\vec{r}_1;t_1) S(\vec{r}_4;t_4)\rangle \langle S(\vec{r}_2;t_2) S(\vec{r}_3;t_3)\rangle. \end{aligned} \tag{8}$$

Each of the three terms on the rhs in Eq. (8) can be further simplified by using Eq. (2) for each of the second-order moments. By substituting this simplified form Eq. (8) in Eq. (7) and after performing spatial and temporal integration of the noise source distribution for the dirac terms $\delta(t_i - t_j)$ and $\delta(\vec{r}_i - \vec{r}_j)$ where $i,j = 1,\ldots,4$ are the indices of the source terms in Eqs. (7) and (8), the expression of $\langle C_{a,b}^2(\tau)\rangle$ reduces to three integral terms:

$$\langle C_{a,b}^2(\tau)\rangle = I(\tau) + J(\tau) + K(\tau). \tag{9}$$

The first integral term $I(\tau)$ is obtained after spatial and temporal integration over source indices $i=2$ and $i=4$. Its expression reduces to $\langle C_{a,b}(\tau)\rangle^2$ by comparison with Eq. (5):

$$\begin{aligned} I(\tau) = & Q^4 \nu^2 \left(\int_{-T_r/2}^{T_r/2} dt \int_{-\infty}^{+\infty} d\vec{r}_1 \int_{-\infty}^{t} dt_1 G(\vec{r}_1,\vec{r}_a;t-t_1) \right. \\ & \left. \times G(\vec{r}_1,\vec{r}_b;\tau+t-t_1) \right) \\ & \times \left(\int_{-T_r/2}^{T_r/2} d\tilde{t} \int_{-\infty}^{+\infty} d\vec{r}_3 \int_{-\infty}^{\tilde{t}} dt_3 G(\vec{r}_3,\vec{r}_a;\tilde{t}-t_3) \right. \\ & \left. \times G(\vec{r}_3,\vec{r}_b;\tau+\tilde{t}-t_3) \right) \\ = & \langle C_{a,b}(\tau)\rangle^2. \end{aligned} \tag{10}$$

The second integral term $J(\tau)$ in Eq. (9) is obtained after spatial and temporal integration over source indices $i=3$ and $i=4$,

$$\begin{aligned} J(\tau) = & Q^4 \nu^2 \int_{-T_r/2}^{T_r/2} dt \int_{-T_r/2}^{T_r/2} d\tilde{t} \left(\int_{-\infty}^{+\infty} d\vec{r}_1 \int_{-\infty}^{t} dt_1 G(\vec{r}_1,\vec{r}_a;t-t_1) \right. \\ & \left. \times G(\vec{r}_1,\vec{r}_a;\tilde{t}-t_1) \right) \left(\int_{-\infty}^{+\infty} d\vec{r}_2 \int_{-\infty}^{t} dt_2 G(\vec{r}_2,\vec{r}_b;\tau+t-t_2) \right. \\ & \left. \times G(\vec{r}_2,\vec{r}_b;\tau+\tilde{t}-t_2) \right). \end{aligned} \tag{11}$$

This expression of the integral term $J(\tau)$ can be simplified by performing the following change of variables $u=t-t_1$, $v=t-t_2$ and $q=t-\tilde{t}$:

$$\begin{aligned} J(\tau) = & Q^4 \nu^2 \int_{-T_r/2}^{T_r/2} dt \int_{-T_r}^{T_r} dq \left(\int_{-\infty}^{+\infty} d\vec{r}_1 \int_{0}^{+\infty} du G(\vec{r}_1,\vec{r}_a;u) \right. \\ & \left. \times G(\vec{r}_1,\vec{r}_a;q+u) \right) \left(\int_{-\infty}^{+\infty} d\vec{r}_2 \int_{0}^{-\infty} dv G(\vec{r}_2,\vec{r}_b;\tau+v) \right. \\ & \left. \times G(\vec{r}_2,\vec{r}_b;q+\tau+v) \right). \end{aligned} \tag{12}$$

By identification with the simplified form of $\langle C_{a,b}(\tau)\rangle$ in Eq. (5), $J(\tau)$ further reduces to

$$J(\tau) = \frac{1}{T_r} \int_{-T_r}^{T_r} dq \langle C_{a,a}(q)\rangle \langle C_{b,b}(q)\rangle, \tag{13}$$

where the autocorrelation functions of the ambient noise signals recorded at receivers a and b are noted respectively as $C_{a,a}(q)$ and $C_{b,b}(q)$.

The third integral term $K(\tau)$ in Eq. (9) is obtained after spatial and temporal integration over the remaining source indices $i=4$ and $i=3$,

$$\begin{aligned} K(\tau) = & Q^4 \nu^2 \int_{-T_r/2}^{T_r/2} dt \int_{-T_r/2}^{T_r/2} d\tilde{t} \left(\int_{-\infty}^{+\infty} d\vec{r}_1 \int_{-\infty}^{t} dt_1 \right. \\ & \left. \times G(\vec{r}_1,\vec{r}_a;t-t_1) G(\vec{r}_1,\vec{r}_b;\tau+\tilde{t}-t_1) \right) \\ & \times \left(\int_{-\infty}^{+\infty} d\vec{r}_2 \int_{-\infty}^{t} dt_2 G(\vec{r}_2,\vec{r}_a;\tilde{t}-t_2) G(\vec{r}_2,\vec{r}_b;\tau+t-t_2) \right). \end{aligned} \tag{14}$$

In a similar way, we can simplify the expression of the integral term $K(\tau)$ in Eq. (14) by performing the following change of variables $u=t-t_1$, $v=\tilde{t}-t_2$ and $q=t-\tilde{t}$:

$$\begin{aligned} K(\tau) = & Q^4 \nu^2 \int_{-T_r/2}^{T_r/2} dt \int_{-T_r}^{T_r} dq \left(\int_{-\infty}^{+\infty} d\vec{r}_1 \int_{0}^{+\infty} du \right. \\ & \left. \times G(\vec{r}_1,\vec{r}_a;u) G(\vec{r}_1,\vec{r}_b;\tau+q+u) \right) \\ & \times \left(\int_{-\infty}^{+\infty} d\vec{r}_2 \int_{0}^{+\infty} dv G(\vec{r}_2,\vec{r}_a;v) G(\vec{r}_2,\vec{r}_b;\tau-q+v) \right). \end{aligned} \tag{15}$$

By identification with the simplified form of $\langle C_{a,b}(\tau)\rangle$ in Eq. (5) we then get

$$K(\tau) = \frac{1}{T_r}\int_{-T_r}^{T_r} dq \langle C_{a,b}(\tau+q)\rangle\langle C_{a,b}(\tau-q)\rangle. \quad (16)$$

Based on Eq. (1), the arrival-time structure of the NCF $\langle C_{a,b}(\tau \pm q)\rangle$ is determined by TDGF $G_{a,b}(\tau \pm q)$. Furthermore, the measured TDGF has a finite duration, i.e., has zero values for running time larger than the temporal length of the retrived TDGF T_{Green} (i.e., $|\tau \pm q| > T_{\text{Green}}$). Hence, using the following approximation,

$$\int_{-T_r}^{T_r} dq \langle C_{a,b}(\tau+q)\rangle\langle C_{a,b}(\tau-q)\rangle \approx G_{a,b}(\tau)^2 \to 0, \quad \text{if } \tau > T_{\text{Green}}, \quad (17)$$

the value of $K(\tau)$ for large correlation time delay $\tau > T_{\text{Green}}$ can be neglected compared to the value of $J(\tau)$ [see Eq. (13)]. Thus using Eqs. (9) and (10) and substituting the result in Eq. (6) and for large correlation time-delay $\tau > T_{\text{Green}}$, the leading term in the expression of the variance of the NCF is $J(\tau)$:

$$[\text{Var}(C_{a,b})]_{\tau > T_{\text{Green}}} = J(\tau) + K(\tau) \approx \frac{\int_{-\infty}^{+\infty} dq \langle C_{a,a}(q)\rangle\langle C_{b,b}(q)\rangle}{T_r}. \quad (18)$$

Equation (18) gives a formulation of the variance *without* making specific assumptions on the particular expression of the TDGF nor for the spectral properties of the noise sources. Indeed, this formulation holds for *any* linear systems as long as the corresponding TDGF has a finite temporal response, which is generally the case due to the presence of attenuation.

Under the assumption of white noise model and finite bandwidth recordings B_ω, the expression of the variance of the NCF given in Eq. (18) can be further reduced. The power spectral densities of receivers a and b are noted respectively $\Phi_{a,a}(\omega)$ and $\Phi_{b,b}(\omega)$. Assuming that the recorded noise has a white spectrum, or after perfoming an preliminar noise whitening operation in practice (see Sec. IV A), the noise spectrum power densities are then a constant in the frequency band of interest: $\Phi_{a,a}(\omega) = C_{a,a}(0)/2B_\omega$ and $\Phi_{b,b}(\omega) = C_{b,b}(0)/2B_\omega$, where B_ω is the frequency bandwidth of interest. Thus, using the Wiener-Khintchine theorem, and assuming that the recording time T_r is sufficiently long so that $\int_{-T_r}^{T_r} \exp(i(\omega+\omega')q)\, dq = \delta(\omega+\omega')$, the following approximation can be made for finite bandwidth recordings:

$$\int_{-T_r}^{T_r} dq \langle C_{a,a}(q)\rangle\langle C_{b,b}(q)\rangle = 4\int_{\omega_c - B_\omega/2}^{\omega_c + B_\omega/2} d\omega \Phi_{a,a}(\omega) \int_{\omega_c - B_\omega/2}^{\omega_c + B_\omega/2} d\omega' \Phi_{b,b}(\omega')\delta(\omega+\omega') = \frac{\langle C_{a,a}(0)\rangle\langle C_{b,b}(0)\rangle}{2B_\omega}, \quad (19)$$

where ω_c is the center frequency of the noise recordings. Hence, for this simplified white noise model, the variance of the NCF reduces to

$$[\text{Var}(C_{a,b})]_{\tau > T_{\text{Green}}} \approx \frac{\langle C_{a,a}(0)\rangle\langle C_{b,b}(0)\rangle}{2B_\omega T_r} = \frac{\int_0^{T_r} dt P(\vec{r}_a;t)^2 \cdot \int_0^{T_r} dt P(\vec{r}_b;t)^2}{2B_\omega T_r}. \quad (20)$$

The simplified expression of the variance $[\text{Var}(C_{a,b})]_{\tau > T_{\text{Green}}}$ given by Eq. (20) is a constant proportional to the product of the total recorded energy by each receiver (which includes the receiver response, noise source amplitude, and potential site effects) and inversely proportional to the recorded time-bandwidth product $T_r B_\omega$ where T_r is the recording time and B_ω is the frequency bandwidth of interest. A similar dependency of the variance on the recorded time-bandwidth product has been previously derived for the case of a finite number of scatterers (or source events) embedded in a homogeneous medium.[11] Furthermore, this simple formulation in Eq. (20) reduces to previous derivations for the case of modal expansions in local diffuse fields.[16,17] For open systems using finite bandwidth Gaussian tone bursts, Eq. (20) corresponds to the leading term in Eq. (41) in Ref. 16. For finite bodies with constant modal density, Eq. (20) corresponds to Eq. (17) in Ref. 17, which is also the leading term in Eq. (38) of the same reference article.

B. Variance of the time derivative of the NCF

As shown in Eq. (1), the arrival-time structure of the TDGF should be estimated in practice using the time derivative of the NCF and not the NCF itself. From Eq. (5) we have

$$\frac{d\langle C_{a,b}(\tau)\rangle}{d\tau} = \nu Q^2 T_r \int_{-\infty}^{+\infty} d\vec{r}_1 \int_0^{+\infty} du G(\vec{r}_1,\vec{r}_a;u) \times \frac{dG(\vec{r}_1,\vec{r}_b;\tau+u)}{d\tau}. \quad (21)$$

The variance $\text{Var}(d(C_{a,b}(\tau)/d\tau))$ of the time derivative of the NCF is defined similarly as in Eq. (6),

$$\text{Var}\left(\frac{dC_{a,b}(\tau)}{d\tau}\right) = \left\langle \left(\frac{d\langle C_{a,b}(\tau)\rangle}{d\tau}\right)^2 \right\rangle - \left\langle \frac{d\langle C_{a,b}(\tau)\rangle}{d\tau} \right\rangle^2, \quad (22)$$

and can be readily estimated following similar derivations presented in the previous section. The main difference is the substitution of terms containing a Green's function with the time-delay variable τ [e.g., $G(\vec{r}_i,\vec{r}_b;\tau+u)$, $i=1,\ldots,4$] by their time derivative [i.e., $dG(\vec{r}_i,\vec{r}_b;\tau+u)/d\tau$]. Hence

$$\text{Var}\left(\frac{dC_{a,b}(\tau)}{d\tau}\right) = DJ(\tau) + DK(\tau). \quad (23)$$

The first integral term $DJ(\tau)$ in Eq. (23) reduces to

$$DJ(\tau) = \frac{1}{T_r}\int_{-T_r}^{+T_r} dq\langle C_{a,a}(q)\rangle\langle DC_{b,b}(q)\rangle, \tag{24}$$

where $\langle DC_{b,b}(q)\rangle$ is the autocorrelation of the *derivative* of the signals recorded at b, $dP(\vec{r}_b;t)/dt$:

$$\langle DC_{b,b}(q)\rangle = \left\langle \int_{-\infty}^{+\infty} dt \frac{dP(\vec{r}_b;t)}{dt}\frac{dP(\vec{r}_b;t+q)}{dt}\right\rangle. \tag{25}$$

The second integral term $DK(\tau)$ in Eq. (23) reduces to

$$DK(\tau) = \frac{1}{T_r}\int_{-T_r}^{T_r} dq\left\langle \frac{dC_{a,b}(\tau+q)}{d\tau}\frac{dC_{a,b}(\tau-q)}{d\tau}\right\rangle. \tag{26}$$

Based on Eq. (1), we can use the following approximation

$$\left\langle \frac{dC_{a,b}(\tau+q)}{d\tau}\right\rangle\left\langle \frac{dC_{a,b}(\tau-q)}{d\tau}\right\rangle \approx G_{a,b}(\tau)^2\delta(p). \tag{27}$$

Hence using similar arguments to the previous section the value of DK for large correlation time delay $\tau > T_{\text{Green}}$ is negligible compare to the expression DJ [see Eq. (24)]. Thus to first order for large correlation time delay $\tau > T_{\text{Green}}$, the leading term in the expression of the variance $\text{Var}(dC_{a,b}(\tau)/d\tau)$ is DJ:

$$\left[\text{Var}\left(\frac{dC_{a,b}(\tau)}{d\tau}\right)\right]_{\tau>T_{\text{Green}}} = \frac{\int_{-\infty}^{+\infty} dq\langle C_{a,a}(q)\rangle\langle DC_{b,b}(q)\rangle}{T_r}. \tag{28}$$

Note that this expression in Eq. (28) does not seem to be symmetric with respect to the role of receivers a and b since only the signal recorded in b is derived. However, if the ambient noise sources are uniformly distributed in space and time, have similar statistics, and the receiver responses are identical, then the signals recorded by receivers a and b have the same characteristics. Note the requirement on the noise source statistics to correctly estimate the TDGF from the NCF. In this case $C_{a,a}(q) \approx C_{b,b}(q)$ and $DC_{a,a}(q) \approx DC_{b,b}(q)$. Thus the roles of receiver a and b in Eq. (28) are indeed interchangeable.

Assuming a white noise model and a finite bandwidth recordings B_ω and using similar derivations done for Eq. (19), the general expression of the variance of the time derivative of the NCF given in Eq. (28) reduces to

$$\left[\text{Var}\left(\frac{dC_{a,b}(\tau)}{d\tau}\right)\right]_{\tau>T_{\text{Green}}} \approx \frac{\langle C_{a,a}(0)\rangle\langle DC_{b,b}(0)\rangle}{2B_\omega T_r}. \tag{29}$$

The simplified expression of the variance of the time derivative of the NCF given by Eq. (29) is a constant proportional to the product of the recorded energy by receiver a and the energy of the time derivative of the signal recorded by receiver b (which includes the receiver responses, site effects, and noise source amplitude) and inversely proportional to the time bandwidth product $T_r B_\omega$.

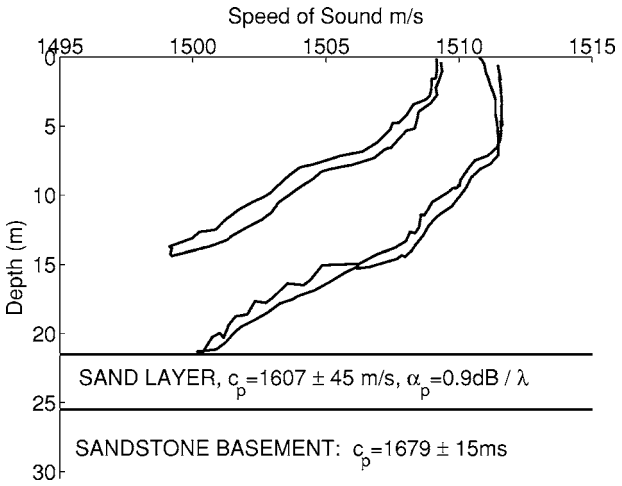

FIG. 1. Model of the range-independent environment in the vicinity of the *NS* array during the ABM95 experiment. The two closest CTD casts were not measured exactly above the location of the arrays but instead in shallower depth (around 15 m, closer to the shoreline) or deeper depth (around 40 m, in the offshore direction from the array). These up and down CTD casts (double lines) are from 0 to 21 m (the water depth at the array location) only.

IV. EXPERIMENTAL RESULTS

A. Experimental measure of the NCF

Ambient noise recordings were collected during the Adaptive Beach Monitoring experiment (ABM 95) near the southern California coast.[9] A bottom horizontal array was deployed along roughly a north-south direction at an average depth of 21 m in a range-independent environment (see Fig. 1). This low frequency (2–750 Hz) hydrophone array had 64 elements with an interelement spacing of $D_{\max}=1.875$ m (equal to half-wavelength spacing at 400 Hz) (see Fig. 2). The sampling frequency was $f_s=1500$ Hz and the array elements had a flat response between approximately 3 and 720 Hz. All array elements were time synchronized. In the

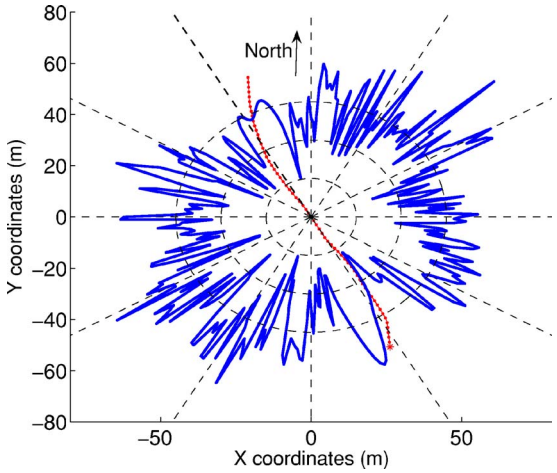

FIG. 2. (Color online) Shape of the bottom array obtained from inversion results.[9] Array elements location are indicated by dots. The origin of the axis coordinates is centered on the middle of the array. The normalized plane wave beamformer output of the array is superimposed on the array shape. Dashed lines shows angular direction with increment of 30°. Three dashed circles indicate the 10-, 20-, and 30-dB level contour levels of the beamformer output.

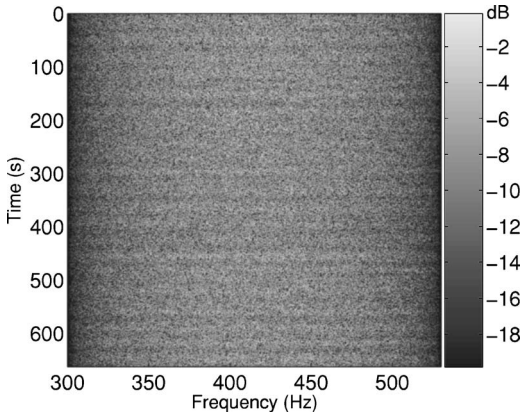

FIG. 3. Normalized spectrogram of 11 min of ambient noise recordings after time-frequency equalization (in the frequency band 300–530 Hz) from JD160 (starting at 0530 UTC), recorded by element 30 of the bottom array (see Fig. 2).

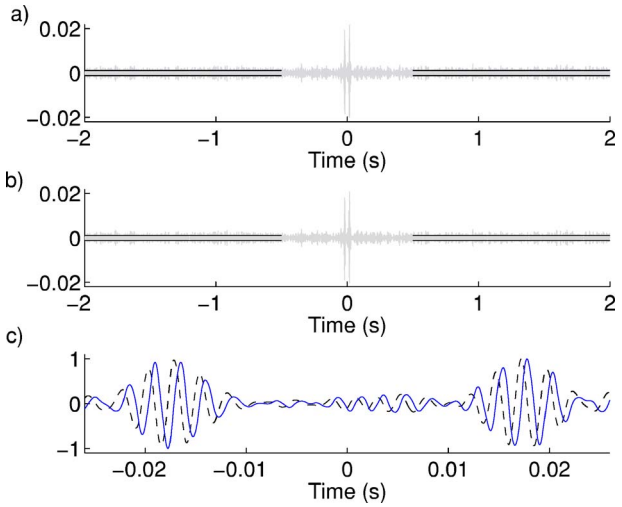

FIG. 4. (Color online) (a) Ambient noise cross-correlation function (NCF) $C_{i,j}(\tau)$, between element $i=30$ and $i=15$ of the bottom array (see Fig. 2). Thirty-three minutes of ambient noise recordings (in the frequency band $B_\omega=300-530$ Hz) were used. The amplitude of the square root of the variance, measured between $0.5<\tau<2s$, is indicated by the black lines. (b) Time derivative of the same NCF which can be used to estimate the arrival time structure of the Green's function. (c) Zoom around the positive and negative arrival times to compare the two time series: the negative time derivative of the NCF $-dC_{i,j}(\tau)/d\tau$ (solid line) and the NCF itself $C_{i,j}(\tau)$ (dashed line). The two time series were resampled at 15 kHz and normalized to their maxima.

vicinity of the array location, the water sound speed at the ocean bottom remained nearly constant at approximately 1495 m/s during this experiment. Details of the experimental setup have been previously presented.[9]

At night, the underwater acoustic ambient noise field was dominated by biological sounds over the 50-Hz to 1-kHz frequency band and the nighttime spectral levels in this band were raised by as much 30 dB over those measured during daylight.[20] The ambient noise field was generated mainly by members of the croaker fish (Sciaenidae) family which migrated at night from the surf zone out to the 21-m water where the bottom hydrophone arrays were located. These noise power spectra exhibit repeatable features of similar intensity throughout the ABM experiment in the 300–700-Hz bandwidth dominated by the croaker sounds consisting of a dominant spectral energy peak between 300 and 530 Hz and a weaker secondary peak between 600 and 700 Hz.[9] Ambient noise data were filtered in the frequency band [300–530 Hz] where the recording amplitude was maximal and the noise field was then created mainly by the distributed croaker fishes. The filtered data were further equalized in the frequency band [300–530 Hz] and a smoothing window was also applied (using a Haning window raised to the power 0.25) in order to render the noise spectrum more uniform before cross correlation. This corresponds to a noise whitening operation for the recorded noise waveforms in the frequency bandwidth of interest. The noise cross-correlation technique works best when the noise distribution is uniform in space and time.[4,7,11,10] Hence data clipping is used subsequently to reduce eventual influence of episodic energetic events (e.g., a loud fish sound close to an hydrophone) which would otherwise dominate the cross correlation. An amplitude threshold of three times the standard deviation of the filtered and equalized noise data was used instead of using a simple but rougher one-bit truncation.[4,14] Figure 3 shows the normalized spectrogram of the 30th array element, in the frequency band 300–530 Hz using 11 min of ambient noise after time-frequency equalization.

Conventional plane wave beamforming was used to verify that the spatial distribution of noise sources surrounding the array was almost uniform. The beamformer output from the noise data was normalized by the beamformer output for the case of uniform superposition of plane waves coming from all directions (i.e., from 0° to 360°) to compensate for the array directivity pattern (or array theoretical response) in the case of a perfectly isotropic noise source distribution. The normalized beamformer output was averaged incoherently across 70 frequencies spanning the whole frequency band 300–530 Hz with a 3.3-Hz increment. The resulting nearly uniform normalized beamformer output shows that the directionality of the croaker sounds was nearly isotropic (see Fig. 2). This confirms previous observations that the bottom hydrophone array was located in the midst of the fish schools.[20] Based on Figs. 2 and 3, the ambient noise field appears to be uniform in space and time in this frequency band. Thus theoretical predictions developed in Sec. II can be used to estimate the variance of the NCF computed from this experimental data set.

Figure 4(a) represents the NCF between the 15th and 30th elements of the north-south array which were separated approximately by 28 m (see Fig. 1). The NCF was obtained using 33 min of ambient noise recordings [see Fig. 3]. The normalized NCF $NC_{a,b}(\tau)$ was computed as the ratio of the NCF and the square root of the recorded energy of each receiver so that the autocorrelation is equal to 1:

$$NC_{a,b}(\tau)=\frac{C_{a,b}(\tau)}{C_{a,a}(0)C_{b,b}(0)}. \tag{30}$$

As expected, the time delays obtained from the NCF are symmetric in time because of the uniform surface noise distribution around the horizontal array (as shown in Fig. 2). Thus, for a pair of receivers $i=30$ and $j=15$, the corresponding NCF $C_{i,j}(\tau)$, for $\tau>0$, is a mirror image of the NCF,

$C_{i,j}(\tau)$, for $\tau<0$, with respect to the time-delay origin $\tau=0$ [see Eq. (1)]. Figure 4(b) represents the time derivative of the NCF displayed in Fig. 4(a). The derivative of the NCF is an antisymmetric function with respect to time, the NCF itself being a symmetric function. The time derivative of the NCF exhibits a clear double-peak structure associated with direct arrival of the TDGF.[9] The ambient noise recorded on the hydrophone array has a relatively small bandwidth B_ω =[300 Hz, 530 Hz]. Hence at first sight the time series of the NCF and its time derivative will look nearly identical. Figure 4(c) compares more closely the two time series $-dC_{i,j}(\tau)/d\tau$ (solid line), which yields the theoretical estimate of the true TDGF, to the NCF $C_{i,j}(\tau)$ (dashed line). The waveforms are similar but with a phase shift (for narrowband signals) corresponding here to a small time delay of 0.5 ms, which yields an error estimate in separation distance of 0.75 m. For a stationary pair separated by large distances with respect to the wavelength, thus yielding large arrival times, this small time delay is often insignificant and within the error bound associated with travel-time measurements. However, for small distances, e.g., 28 m in this case or roughly 7.5 wavelengths, this small time delay can cause a significant error in travel-time measurements. Thus, using the derivative of the NCF yields a crucial difference for the precise measurement required for array element localization[9] or small-scale tomography.

The time derivative of the NCF clearly shows the direct arrivals of the TDGF between two array elements; however, other multipath arrivals of the TDGF do not appear as clearly. This is most likely due to the multiple interaction with the moving free surface and the high attenuation bottom for the coherent components of the noise field propagating between the receivers along high angle paths. Indeed, in the presence of environmental fluctuation, the contribution of these noise components to the time-averaged NCF may not average coherently over long recording time period, i.e., T_r in the order of tenths of minutes. Thus the high angle paths may not emerge as reliably over time from the time-averaged NCF. Furthermore, even though the dominant noise sources (croakers) are uniformly distributed around the array, they may be quite directional since the croakers are typically located close to the hard ocean bottom (thus approaching baffled sources). Hence the shading introduced by the directionality of the noise sources may also further reduce the emergence of the high angle paths in the NCF.[7,8]

B. Experimental measure of the variance of the NCF

Following the theoretical discussions in Sec. II, the variance of the NCF was computed for long time-delay 0.5 s $\leqslant|\tau|\leqslant$2 s, much larger than the maximal travel time between array elements which is $(N-1)D_{\max}/c_0\approx 0.08$ s, where $N=64$ and $D_{\max}=1.875$ m. For instance, the square root of the variance is indicated by a thick line for respectively the NCF and its time derivative in Figs. 4(a) and 4(b), corresponding to a receiver separation distance of 28 m and a recording time $T_r=33$ min. To investigate the variations of the variance of the NCF, the experimental NCF was computed for six receiver pairs spaced from 1.82 to 27.65 m

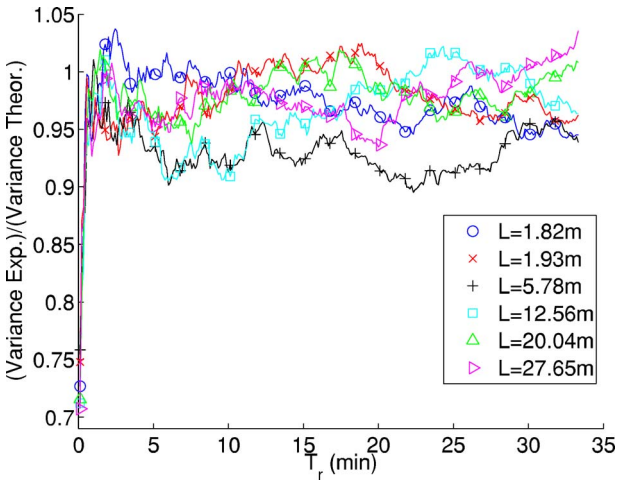

FIG. 5. (Color online) Ratio of the experimental measurements of the variance and the simplified theoretical predictions for the variance of the NCF given by Eq. (20) for increasing recording time T_r and for six receiver pairs with increasing separation distance L. This ratio is $\mathrm{Var}(C_{a,b})\times(2B_\omega^E T_r)/(\langle C_{a,a}(0)\rangle\langle C_{b,b}(0)\rangle)$ for two receivers a and b. The effective bandwidth was set to $B_\omega^E\approx 180$ Hz.

(using element 30 as the first receiver and by using different hydrophones as the second receivers) for increasing recording time from 6.6 s to 33 min by increments of 6.6 s.

Since the ambient noise recordings were windowed in the frequency bandwidth [300–530 Hz], the effective frequency bandwidth B_ω^E was indeed smaller: $B_\omega^E\approx 180$ Hz for most receiver pairs. Figure 5 compares the ratio of the experimental measurements of the variance of the NCF and the theoretical predictions for the variance of the NCF given by Eq. (20) for increasing recording time T_r and for each of the six receiver pairs using the effective bandwidth B_ω^E. The ratio $\mathrm{Var}(C_{a,b})\cdot(2B_\omega^E T_r)/(\langle C_{a,a}(0)\rangle\langle C_{b,b}(0)\rangle)$ remains close to one for all receiver pairs and recording time T_r larger than 1 min. For this short bandwidth, the amplitudes of the time derivative of NCF and of the NCF itself were almost identical (see Fig. 4). The ratio between the variance of the time derivative of the NCF and the corresponding theoretical predictions given by Eq. (29) yielded identical curves as in Fig. 5, all very close to 1. The theoretical predictions deviate from the experimental results for a small recording time-window length T_r (below 1 min here), which is insufficient for the time averaging for the ambient noise statistics to converge. Furthermore, the deviations of the noise source distributions from the case of an isotropic distribution may also affect the results.[9]

V. CONCLUSIONS

Theoretical predictions of the variance of the ambient noise cross-correlation function (NCF) between two receivers (and of its time derivative) have been derived and were simplified assuming a finite temporal length for the Green's function and a white noise nodel. The dominant term for simplified expression of the variance of the NCF is a constant proportional to the product of the recorded energy by both receivers and inversely proportional to the time-bandwidth product $T_r B_\omega$ where T_r is the recording time and B_ω is the frequency bandwidth of the recordings [see Eq.

(20)]. The expression of the recorded energy includes the receiver responses, site effects, and noise source amplitude. The variance of the time derivative of the NCF has a similar dependency but the recorded energy by one of the receivers is now replaced by the energy of the time derivative of the recorded signals instead [see Eq. (29)]. These simple analytic formulas provide a way to quantify the signal-to-noise ratio of the NCF and its time derivative.[9,13] A good agreement with experimental measurement of the variance of the NCF was found for ocean ambient noise recordings in shallow water in the frequency band [300–530 Hz] for receiver separations up to 28 m.

For such short separation distances between elements and strong bottom absorption, it was mentioned in Sec. III A that multipath arrivals of the NCF are not likely to be observed since they should have indeed a weak amplitude. Provided there is a simple estimate of the amplitude of the multipath arrivals (e.g., using a ray code[18]), the theoretical predictions given by Eq. (20) can be used to estimate the minimal duration of the noise recordings for the variance of the NCF to fall below a certain detection threshold for those arrivals. For the ABM95 environment and noise statistics the recording time should amount to several hours in order to have sufficient averaging time for the weak multipath arrivals to emerge from the NCF. However, fluctuations of the environment (e.g., tides, moving free surface, change of water sound speeds) render the acoustic paths nonstationary over such long durations and thus would prevent the coherent emergence of these multipath arrivals. On the other hand, for a more stable environment such as the earth crust in seismology applications, the theoretical predictions given by Eq. (20) can help to specify the amount of averaging necessary to recover both surface waves as well as body waves from seismic noise recordings.[13,14]

ACKNOWLEDGMENTS

This works was supported by the Office of Naval Research. We thank the two anonymous reviewers for their constructive comments.

[1]J. Rickett and J. Claerbout, "Acoustic daylight imaging via spectral factorization: Helioseismology and reservoir monitoring," The Leading Edge **18**, 957–960 (1999).

[2]O. I. Lobkis and R. L. Weaver, "On the emergence of the green's function in the correlations of a diffuse field," J. Acoust. Soc. Am. **110**, 3011–3017 (2001).

[3]R. L. Weaver and O. I. Lobkis, "Elastic wave thermal fluctuations, ultrasonic waveforms by correlation of thermal phonon," J. Acoust. Soc. Am. **113**, 2611–2621 (2003).

[4]E. Larose, A. Derode, M. Campillo, and M. Fink, "Imaging from one-bit correlations of wideband diffuse wavefields," J. Appl. Phys. **95**, 8393–8399 (2004).

[5]A. E. Malcolm, J. A. Scales, and B. van der Tiggelen, "Retrieving the green function from diffuse equipartitioned waves," Phys. Rev. E **70**, 015601(R) (2004).

[6]R. L. Weaver and O. I. Lobkis, "Diffuse fields in open systems and the emergence of the greens function," J. Acoust. Soc. Am. **116**, 2731–2734 (2004).

[7]P. Roux, W. A. Kuperman, and the NPAL Group, "Extracting coherent wavefronts from acoustic ambient noise in the ocean," J. Acoust. Soc. Am. **116**, 1995–2003 (2004).

[8]K. G. Sabra, P. Roux, and W. A. Kuperman, "Arrival-time structure of the time-averaged ambient noise cross-correlation function in an oceanic waveguide," J. Acoust. Soc. Am. **117**, 164–174 (2005).

[9]K. G. Sabra, P. Roux, A. M. Thode, G. L. D'Spain, W. S. Hodgkiss, and W. A. Kuperman, "Using ocean ambient noise for array self-localization and self-synchronization," IEEE J. Ocean. Eng. (unpublished).

[10]N. M. Shapiro and M. Campillo, "Emergence of broadband rayleigh waves from correlations of the ambient seismic noise," Geophys. Res. Lett. **31**, L07614 (2004).

[11]R. Snieder, "Extracting the green's function from the correlation of coda waves: A derivation based on stationary phase," Phys. Rev. E **69**, 046610 (2004).

[12]K. Wapenaar, "Retrieving the elastodynamic greens function of an arbitrary inhomogeneous medium by cross correlation," Phys. Rev. Lett. **93**, 254301 (2004).

[13]K. G. Sabra, P. Gerstoft, P. Roux, W. Kuperman, and M. C. Fehler, "Extracting time-domain greens function estimates from ambient seismic noise," Geophys. Res. Lett. **32**, L03310 (2005).

[14]N. M. Shapiro, M. Campillo, L. Stehly, and M. Ritzwoller, "High-resolution surface-wave tomography from ambient seismic noise," Science **29**, 1615–1617 (2005).

[15]P. Roux, K. Sabra, W. Kuperman, and A. Roux, "Ambient noise cross-correlation in free space: theoretical approach," J. Acoust. Soc. Am. **117**, 79–84 (2005).

[16]R. L. Weaver and O. I. Lobkis, "Fluctuations in diffuse field-field correlations and the emergence of the green's function in open systems," J. Acoust. Soc. Am. **117**, 3432–3439 (2005).

[17]R. L. Weaver and O. I. Lobkis, "The mean and variance of diffuse-field correlations in finite bodies," J. Acoust. Soc. Am. (unpublished).

[18]F. B. Jensen, W. A. Kuperman, M. B. Porter, and H. Schmidt, *Computational Ocean Acoustics* (AIP, New York, 2000).

[19]M. Buckingham, in *Noise in Electronic Devices and Systems*, edited by E. Horwood (Wiley, New York, 1983), p. 30.

[20]G. L. D'Spain, L. Berger, W. A. Kuperman, and W. S. Hodgkiss, "Summer night sounds by fish in shallow water," in *Proc. Int. Conf. on Shallow-Water acoustics* (China Ocean Press, Beijing, 1997), pp. 379–384.